J|A|C|S ARTICLES

Published on Web 02/11/2009

Dynamics of Localized Charges in Dopamine-Modified TiO_2 and their Effect on the Formation of Reactive Oxygen Species

Nada M. Dimitrijevic,*,†,‡ Elena Rozhkova,† and Tijana Rajh†

Center for Nanoscale Materials, and Chemical Sciences and Engineering Division, Argonne National Laboratory, Argonne, Illinois 60439

Received September 30, 2008; E-mail: Dimitrijevic@anl.gov

Abstract: Modification of TiO_2 nanoparticles with dopamine enables harvesting of visible light and promotes spatial separation of charges. The formation of reactive oxygen species (OH, $^1O_2$, O_2^-, HO_2, H_2O_2) upon illumination of TiO_2/dopamine was studied using complementary spin-trap EPR and radical-induced fluorescence techniques. The localization of holes on dopamine suppresses oxidation of adsorbed water molecules at the surface of nanoparticles, and thus formation of OH radicals. At the same time, dopamine does not affect electronic properties of photogenerated electrons and their reaction with dissolved oxygen to produce superoxide anions. Superoxide anions are proposed to generate singlet oxygen through dismutation reaction, resulting in a low yield of $^1O_2$ detected.

Introduction

The bioinorganic hybrids made by connecting inorganic nanostructures (nanoparticles, nanorods) to biomolecules (proteins, DNAs) and the resulting conjugates combine the properties of both materials, i.e., the electronic structure and characteristics of the nanocrystallites and the biomolecular function of the surface-attached entities.[1] With the appropriate design, these conjugates can be introduced into cells to initiate intracellular processes or biochemical reactions.[2−5] We have recently developed hybrid nanocomposites which electronically link photoactive TiO_2 nanoparticles to DNA and biotin/avidin and have shown efficient separation of photogenerated charges in these conjugates, that is, electrons localize on TiO_2 and holes on DNA or protein.[6,7] These initial results present an opportunity to use titania-based conjugates for medical applications. The advantage of using titania-based conjugates lies in the nontoxicity of TiO_2 and in its biocompatibility with both primary and cancer cells.[8] Upon excitation, due to the efficient separation of photogenerated charges in TiO_2, redox chemical reactions with surrounding and/or attached biomolecules can yield cytotoxicity. Namely, it is well-known that photoexcitation of TiO_2 in an aqueous solution results in the formation of various reactive oxygen species (ROS) such as hydroxyl (OH) and peroxy (HO_2) radicals, superoxide anions (O_2^-), and hydrogen peroxide (H_2O_2).[9−12] Moreover, the formation of singlet oxygen ($^1O_2$) was recently confirmed by measuring phosphorescence of $^1O_2$ at 1260 nm upon excitation of TiO_2 nanoparticles of dimensions larger than 10 nm.[13] OH radicals are formed in reaction of photogenerated holes with surrounding water and to a lesser extent as a result of radical- or photoreactions of hydrogen peroxide or superoxide,[14] while O_2^- is formed in the reaction of photogenerated electrons with oxygen molecules. The formation of singlet oxygen on bare TiO_2 particles was proposed to undergo three different mechanisms: (i) reaction of superoxide anion with holes,[13] (ii) water-induced dismutation of two superoxide anions which results in at least partially excited oxygen molecules,[15] and (iii) energy transfer as a result of electron−hole recombination.[16] Additionally, $^1O_2$ was not detected upon illumination of anatase particles <10 nm, allegedly because of the insufficient charge separation in small-sized particles.[13] Without going into the details of actual mechanisms,[17] the major reactions that result in the formation of ROS upon illumination of bare TiO_2 are shown as simplified eqs 1−6.

† Center for Nanoscale Materials.
‡ Chemical Sciences and Engineering Division.

(1) Niemeyer, C. M. *Angew. Chem., Int. Ed.* **2001**, *40*, 4128–4158.
(2) You, C.-C.; Chompoosor, A.; Rottelo, V. M. *Nanotoday* **2007**, *2*, 34–43.
(3) Tkachenko, A. G.; Xie, H.; Coleman, D.; Glomm, W.; Ryan, J.; Anderson, M. F.; Franzen, S.; Feldheim, D. L. *J. Am. Chem. Soc.* **2003**, *125*, 4700–4701.
(4) Paunesku, T.; Rajh, T.; Wiederrecht, G.; Maser, J.; Vogt, S.; Stojicevic, N.; Protic, M.; Lai, B.; Oryhon, J.; Thurnauer, M.; Woloschak, G. *Nat. Mater.* **2003**, *2*, 343–346.
(5) Clarke, S. J.; Hollmann, C. A.; Zhang, Z.; Suffern, D.; Bradforth, S. E.; Dimitrijevic, N. M.; Minarik, W. G.; Nadeau, J. L. *Nat. Mater.* **2006**, *5*, 409–417.
(6) Rajh, T.; Saponjic, Z.; Liu, J.; Dimitrijevic, N. M.; Scherer, N. F.; Vega-Arroyo, M.; Zapol, P.; Curtiss, L. A.; Thurnauer, M. C. *Nano Lett.* **2004**, *4*, 1017–1023.
(7) Dimitrijevic, N. M.; Saponjic, Z. V.; Rabatic, B. M.; Rajh, T. *J. Am. Chem. Soc.* **2005**, *127*, 1344–1345.
(8) Carbone, R.; Marangi, I.; Zanardi, A.; Giorgetti, L.; Chierici, E.; Berlanda, G.; Podesta, A.; Fiorentini, F.; Bongiorno, G.; Piseri, P.; Pelicci, P. G.; Milani, P. *Biomaterials* **2006**, *27*, 3221–3229.
(9) Hoffmann, M. R.; Martin, S. T.; Choi, W.; Bahnemann, D. W. *Chem. Rev.* **1995**, *95*, 69–96.
(10) Mills, A.; Le Hunte, S. *J. Photochem. Photobiol., A* **1997**, *108*, 1–35.
(11) Schwarz, P. F.; Turro, N. J.; Bossmann, S. H.; Braun, A. M.; Wahab, A.-M. A. A.; Durr, H. *J. Phys. Chem. B* **1997**, *101*, 7127–7134.
(12) (a) Nosaka, Y.; Komori, S.; Yawata, K.; Hirakawa, T.; Nosaka, A. Y. *Phys. Chem. Chem. Phys.* **2003**, *5*, 4731–4735. (b) Nosaka, Y.; Natusi, H.; Sasagawa, M.; Nosaka, A. Y. *J. Phys. Chem. B* **2006**, *110*, 12993–12999.
(13) Daimon, T.; Nosaka, Y. *J. Phys. Chem. C* **2007**, *111*, 4420–4424.
(14) Tachikawa, T.; Majima, T. *J. Fluoresc.* **2007**, *17*, 727–738.
(15) Khan, A. U. *Int. J. Quantum Chem.* **1991**, *39*, 251–267.
(16) Janczyk, A.; Krakowska, E.; Stochel, G.; Macyk, W. *J. Am. Chem. Soc.* **2006**, *128*, 15574–15575.
(17) Nakamura, R.; Nakato, Y. *J. Am. Chem. Soc.* **2004**, *126*, 1290–1298.

$$TiO_2 + h\nu \rightarrow e_{tr}^- + h_{surf}^+ \quad (1)$$

$$h_{surf}^+ + H_2O \rightarrow OH + H^+ \quad (2)$$

$$e_{tr}^- + O_2 \rightarrow O_2^- \quad (3)$$

$$O_2^- + H^+ \leftrightarrow HO_2,\ pK = 4.8 \quad (4)$$

$$2HO_2\ (\text{or } 2O_2^-) \rightarrow H_2O_2\ (\text{or } O_2) + {}^1O_2 \quad (5)$$

$$O_2^- + h_{surf}^+ \rightarrow {}^1O_2 \quad (6)$$

The differences in lifetimes, i.e. reactivity, of ROS determine the distance they can diffuse in a cell; thus, for short-lived ROS like OH and $^1O_2$, a cell response of interest might be initiated by products of the primary reactions of these species with neighboring molecules.[18] On the other hand, relatively long-lived species such as O_2^-/HO_2 and H_2O_2 have been shown to diffuse over long distances, affecting neighboring cells.[19] The design of bioinorganic conjugates for photodynamic therapy-type medical applications would thus be driven by a "spatially resolved"[18] response. Furthermore, the modification of the titania surface, which is a necessary step in construction of bio-TiO_2 hybrids, may affect the formation and yield of ROS. Even though the cytotoxicity of photoexcited bare TiO_2 (mainly mixed-phase Degussa P25) is largely studied,[20] there are very few reports on the formation of ROS from surface-modified TiO_2; specifically, singlet oxygen and/or superoxide anions were detected in cyanuric acid-modified[16] or carotenoid-modified TiO_2.[21]

The strategy for attaching biomolecules on the surface of TiO_2 is to utilize the ability of oxygen-containing substituents, such as carboxy, hydroxy, and phosphoric acid groups, to bind to the surface of nanoparticles.[22−24] Our approach in construction of bio-TiO_2 hybrids is to use dopamine, which due to two OH groups in the ortho position makes a strong bidentate complex with coordinatively unsaturated Ti atoms at the surface of nanoparticles.[23] Furthermore, when DNA or proteins were covalently bound to dopamine, it was found that dopamine acts as a conductive lead between TiO_2 nanocrystallites and biomolecules, allowing transport of photogenerated holes to biomolecules.[6,7] For possible medical applications of such hybrids, it is important to determine which ROS are formed, as they can initiate different mechanisms of cytotoxicity. The formation of OH radicals and singlet oxygen with their relatively low diffusion length (estimated to be <20 nm for OH and 20−220 nm for $^1O_2$ in a cell)[18,25] may promote necrosis. On the other hand, O_2^-/HO_2 and H_2O_2 may induce apoptosis. Because ROS are formed through redox reactions at the surface of nanoparticles, the attachment of surface modifiers such as dopamine can affect their overall yield.

With the aim to investigate the effects of the surface modifier on the formation of ROS we have studied dopamine-modified TiO_2 (TiO_2/DA) using electron paramagnetic resonance (EPR) technique of spin probe/trap, as well as fluorescent probes for singlet oxygen and superoxide anions. For this purpose 4.5 nm anatase particles were used. The results obtained for bare particles, particles partially modified with dopamine, and TiO_2 with full coverage of coordinatively unsaturated Ti surface sites with dopamine are presented in this paper.

Experimental Section

Materials. Dopamine hydrochloride (Sigma), DA; spin traps: 2,2,6,6-tetramethylpiperidine-1-oxyl (Aldrich), TEMPOL free radical, 2,2,6,6-tetramethylpiperidine (Aldrich), TEMP, and α-(4-pyridyl-*N*-oxide)-*N*-*tert*-butylnitrone (Aldrich), POBN, were all analytical grade and used as received, without further purification. Fluorescent probes: dihydrorhodamine 123, DHR-123, and singlet oxygen sensor green, SOSG, were purchased from Invitrogen, and kept at −80 °C. The stock solutions in methanol were prepared just prior to use. Antibody (IgG) from human serum was purchased from Sigma. The conjugation of IgG onto TiO_2/DA nanocrystallites was performed by a condensation reaction of amino and carboxyl groups via succinimide,[26] in a process similar to one described previously for the coupling of DNA to TiO_2 nanoparticles.[6] The conjugation resulted in ∼1 IgG per particle.

The preparation and characterization of 4.5 nm TiO_2 nanoparticles is described elsewhere,[27] and only outlined herein. The seeds of colloidal TiO_2 were prepared by dropwise addition of titanium(IV) chloride (99.0% Fluka) to cooled water, while slow growth of the particles was achieved by dialysis against water until the pH of the solution reached pH 3.5. Colloidal solutions of particles were kept at 4 °C for at least six months because the aging improved the crystallinity.

Techniques. X-band continuous wave (CW) and pulsed EPR experiments were conducted on a Bruker Elexsys E580 spectrometer equipped with an Oxford CF935 helium flow cryostat with an ITC-5025 temperature controller. Pulsed EPR measuremets were conducted at temperatures from 4 to 100 K, while CW measurements using spin traps were performed at room temperature. For EPR-direct studies of photogenerated charges, solutions were degassed with Ar, for spin trap measurements they were degassed with oxygen, Ar, or exposed to air. The *g* factors were calibrated for homogeneity and accuracy by comparison to a coal standard, $g = 2.00285 \pm 0.00005$. A Bruker weak pitch #150W152 reference sample was applied for quantitative analysis, in combination with a known concentration of TEMPOL radical. The receiver gain and number of scans were adjusted to every spectrum of a particular sample to enable comparisons at a reasonable signal-to-noise ratio. As the area under the absorption curve is proportional to the number of unpaired spins, the results of double integration of the first derivative EPR signals were compared with those of the standards. The accuracy of the measurements is charged with an error of 20%.

Samples were excited either with 355 nm photons from a frequency-tripled Nd:YAG laser (power 6 mJ), or by using a 300-W Xe lamp (ILC) and appropriate filters. A two-pulse sequence ($\pi/2-\tau-\pi-\tau$-echo) was used to measure spin−spin relaxation times, T_2, by changing the durations of the first ($\pi/2$) and second (π) pulse. A three-pulse inversion−recovery experiment ($\pi-T-\pi/2-\tau-\pi-\tau$-echo) was employed for measuring spin−lattice relaxation times, T_1. The delay (T) after the first inversion pulse was varied, while τ was kept constant. Multiple scans were performed in order to

(18) Redmond, R. W.; Kochevar, I. E. *Photochem. Photobiol.* **2006**, *82*, 1178–1186.
(19) Panus, P. C.; Radi, R.; P. H.; Chumley, P. H.; Lillard, R. H.; Freeman, B. A. *Free Radical Biol. Med.* **1993**, *14*, 217–223.
(20) See for example:(a) Matsunaga, T.; Tomoda, R.; Nakajima, T.; Wake, H. *FEMS Microbiol. Lett.* **1985**, *29*, 211–214. (b) Cai, R.; Kubota, Y.; Shuin, T.; Sakai, H.; Hashimoto, K.; Fujishima, A. *Cancer Res.* **1992**, *52*, 2346–2348. (c) Maness, P.-C.; Smolinski, S.; Blake, D. M.; Huang, Z.; Wolfrum, E. J.; Jacoby, W. A. *Appl. Environ. Microbiol.* **1999**, *65*, 4094–4098. (d) Uchino, T.; Tokunaga, H.; Ando, M.; Utsumi, H. *Toxicol. in Vitro* **2002**, *16*, 629–635.
(21) Konovalova, T. A.; Lawrence, J.; Kispert, L. D. *J. Photochem. Photobiol., A* **2004**, *162*, 1–8.
(22) O'Regan, B.; Gratzel, M. *Nature* **1991**, *353*, 737–740.
(23) Rajh, T.; Chen, L. X.; Lukas, K.; Liu, T.; Thurnauer, M. C.; Tiede, D. M. *J. Phys. Chem. B* **2002**, *106*, 10543–10552.
(24) Duncan, W. R.; Prezhdo, O. V. *Annu. Rev. Phys. Chem.* **2007**, *58*, 143–184.
(25) Schweitzer, C.; Schmidt, R. *Chem. Rev.* **2003**, *103*, 1685–1757.
(26) Hermanson, G. T. *Bioconjugate Techniques*; Academic Press: San Diego, CA, 1996.
(27) Rajh, T.; Tiede, D. M.; Thurnauer, M. C. *J. Non-Cryst. Solids* **1996**, *207*, 815–820.

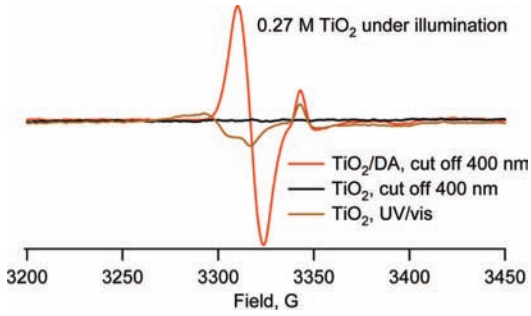

Figure 1. CW EPR spectra of Ar-saturated aqueous solution of TiO_2/DA (red line) and bare TiO_2 (black line) under visible light excitation (Xe lamp, cut-off filter 400 nm). Concentration of TiO_2 was 0.27 M, and added dopamine, 85 mM, pH 3.5. For comparison, a spectrum of bare titania particles illuminated under UV light (no filter) is present (brown line). Temperature 5.2 K, microwave power 2.0 mW, modulation amplitude 5 G.

improve the signal-to-noise ratio. The spin−lattice relaxation signals in the experiments reported here were fitted with a biexponential curve. We considered the initial fast decay to be due to cross relaxation and determined the time T_1 from the tail of the recovery signal. Actinometry was carried out in quartz tubes in an EPR cavity using phenylglyoxylic acid photodecarboxylation.[28]

Absorption spectra were measured on a UV/visible spectrometer (Shimadzu, UV-1601), while fluorescence spectra were measured on a QuantaMaster Luminescence spectrometer (PTI). Solutions with fluorescent probes were illuminated with a 300-W Xe lamp (ILC), using 360 nm band-pass and IR filters. Solutions were placed into a cuvette, and fluorescence was measured after time intervals of illumination.

Results and Discussion

Efficient Charge Separation. Band-gap excitation of TiO_2 (with photon energies ≥3.2 eV) results in ejection of electrons from valence to conduction band. As was determined previously by low-temperature EPR measurements,[29,30] electrons localize in the titania lattice at shallow trapping sites, $(Ti^{3+})_{latt}$, while holes localize at the surface of particles as oxygen-centered radicals $(Ti^{4+}O\bullet)_{surf}$, reaction 1.

$$TiO_2 + h\nu \rightarrow e_{tr}^-[(Ti^{3+})_{latt}] + h_{surf}^+[(Ti^{4+}O\bullet)_{surf}] \qquad (1a)$$

Modification of TiO_2 nanoparticles with dopamine promotes spatial separation of photogenerated charges; localization of holes on dopamine and electrons in TiO_2 is well established,[23] reaction 7.

$$TiO_2/DA + h\nu \rightarrow e_{tr}^-[(Ti^{3+})_{latt}]/DA^+ \qquad (7)$$

Additionally, TiO_2/DA enables absorption of a visible part of the solar spectrum. Figure 1 presents CW EPR spectra obtained upon excitation of TiO_2/DA with light energies <3.2 eV. The signal with $g = 2.0036$ corresponds to dopamine cation radical, DA^+, and the signal with $g_\perp = 1.988$, to $(Ti^{3+})_{latt}$. The same radicals are observed when TiO_2/DA is excited by UV light, as both electrons and holes localize on thermodynamically preferred sites, electrons in the lattice of particles, and holes on dopamine. On the other hand, when bare particles are illuminated with light energies <3.2 eV, charges cannot be formed because photons do not possess enough energy to excite electrons from the valence to the conduction band of TiO_2 (black line in Figure 1). These data are consistent with the existence of a charge-transfer complex in dopamine-modified TiO_2 nanoparticles that promotes extended charge separation both upon visible and UV excitation. Moreover, due to the spatial separation of photogenerated charges in TiO_2/DA charge-transfer complex, charge recombination is suppressed. For example, we have found for $(Ti^{3+})_{latt}$ that the number of spins (concentration of trapped electrons) increases quite significantly from 1.0×10^{15} spins/cm^3 for bare TiO_2 under UV/vis illumination to 1.6×10^{15} spins/cm^3 and 1.8×10^{15} spins/cm^3 for TiO_2/DA under visible or UV/vis light, respectively. The EPR spectra were taken under continuous illumination; thus, the intensities of the signals and calculated number of spins correspond to the steady-state concentrations of products, in our case ruled by the formation and recombination of electrons and holes.

In order to obtain more insight into the properties of photogenerated charges in the TiO_2/DA charge-transfer complex, we performed pulsed EPR experiments that through spin−spin, T_2, and spin−lattice, T_1, relaxation times provide information on hyperfine and dipolar interactions, coupling of electron spin with nuclear spin of surrounding nuclei, as well as phonon interactions. By comparing spin dynamics for bare and dopamine-modified TiO_2 nanoparticles, we sought to distinguish properties of localized charges that can have impact on redox reactions on the surface of particles. The field-swept echo spectra recorded upon monochromatic UV excitation, $\lambda = 355$ nm, 6 mJ, of Ar-saturated aqueous solution of bare TiO_2 and TiO_2/DA nanocrystallites at liquid He temperature are presented in Figure 2a. Both T_2 and T_1 relaxation times were determined at the resonance field corresponding to particular radicals, DA^+ or $(Ti^{3+})_{latt}$, for dopamine-modified, and $(Ti^{4+}O\bullet)_{surf}$ or $(Ti^{3+})_{latt}$ for bare particles, respectively. We have found that the spin−spin relaxation time of carbon-centered radical DA^+ (determined to be 1.2 μs at 7 K) is faster than that for holes localized on the surface of bare TiO_2 in the form of oxygen-centered radicals ($T_2 = 2.2$ μs at 7 K),[31] suggesting dephasing influenced by strong hyperfine and dipolar interactions, Figure 2b. The well-resolved amplitude modulations observed in decay of DA^+ are due to the coupling of electron spin with nuclear spin of hydrogen atoms of dopamine. Similarly, we have found that the spin−lattice relaxation T_1 differs significantly for holes localized on dopamine compared to the holes on the surface of bare particles. Curves c (for trapped electrons) and d (for trapped holes) of Figure 2 contain the results of a biexponential fit of the saturation recovery signal measured up to 70 K and presented as dependence of $1/T_1$ on the temperature (T). For bare particles, the temperature dependence of $1/T_1$ for $(Ti^{4+}O\bullet)_{surf}$ and $(Ti^{3+})_{latt}$ follows the same pattern. Namely, going from low to high temperatures, the exponent of temperature dependence changes from 1 ($1/T_1 \approx T^1$ at $T < 10$ K) to approximately 6 ($1/T_1 \approx T^6$ at $T > 10$ K). The main mechanism of the energy relaxation in crystals is a modulation of the electric crystal field by lattice vibrations (phonons) transmitted to the electron magnetic moment by the spin−orbit coupling.[32] As we have shown previously for trapped electrons in differently shaped anatase nano-objects,[31] at temperatures below 10 K relaxation

(28) Kuhn, H. J.; Braslavsky, S. E.; Schmidt, R. *Pure Appl. Chem.* **2004**, *76*, 2105–2146.
(29) (a) Howe, R. F.; Gratzel, M. *J. Phys. Chem.* **1985**, *89*, 4495–4499. (b) Howe, R. F.; Gratzel, M. *J. Phys. Chem.* **1987**, *91*, 3906–3909.
(30) Berger, T.; Sterrer, M.; Diwald, O.; Knozinger, E.; Panayotov, D.; Thompson, T. L.; Yates, Jr., J. T. *J. Phys. Chem. B* **2005**, *109*, 6061–6068.
(31) Dimitrijevic, N. M.; Saponjic, Z. V.; Rabatic, B. M.; Poluektov, O. G.; Rajh, T. *J. Phys. Chem. C* **2007**, *111*, 14597–14601.
(32) Standley, K. J.; Vaughan, R. A. *Electron Spin Relaxation Phenomena in Solids*; Adam Hilger Ltd.: London, 1969.

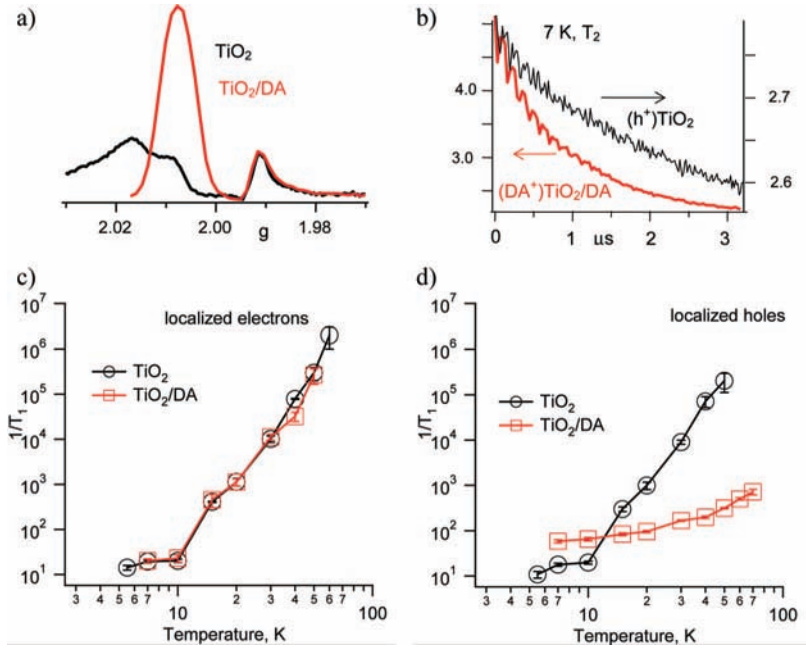

Figure 2. Pulsed EPR measurements upon 355 nm excitation of TiO_2 and TiO_2/DA particles. (a) Field-swept echo spectra. The first ($\pi/2$) and second (π) pulse durations were 16 and 32 ns, respectively. Changing the time between pulses (t) from 100 to 400 ns did not affect spectra. (b) Spin−echo amplitude decay at 7 K, in 10^6 arbitrary units, measured at resonant field of trapped holes for bare, or DA^+ for dopamine-modified TiO_2, obtained after applying two-pulse sequence. Effect of temperature on spin−lattice relaxation times for localized (c) electrons and (d) holes.

is characteristic of the direct one-phonon resonant process, while at $T > 10$ K the relaxation corresponds to nonresonant Raman process. The dependence on temperature, such as T^6, suggests a relaxation mechanism through phonon-modulated hyperfine coupling.[33] The same spin−lattice relaxation observed for surface-trapped holes and lattice-trapped electrons in bare particles implies the same dynamical coupling to the crystal field. On the other hand, our results show that holes localized on dopamine are not coupled to the anatase crystal field, instead behaving as separate entities. The temperature dependence of $1/T_1$ for DA^+/TiO_2 is presented in Figure 2d. The relaxation is dominated by direct process at $T < 20$ K, while at higher temperatures Raman process with $1/T_1 \approx T^{1.5}$ was observed. This low-power dependence is probably due to the intrinsic relaxation characteristic for organic radicals.[34] This further confirms the effectiveness of TiO_2/DA charge-transfer complex. Although all measurements were conducted at cryogenic temperatures (which corresponds to < ps events at room temperature), they suggest that localization of holes on attached dopamine may affect oxidation reactions, specifically the formation of OH radicals, reaction 2, as the redox potential of DA^+/TiO_2 sites ($E^0 < 1.0$ V[35]) is more negative than the potential of valence band or surface-trapped holes of TiO_2 ($E_{VB}{}^0 = 2.8$ V[9]).

At the same time, we have found that electronic and spin properties of $(Ti^{3+})_{latt}$ are unaffected by attached dopamine, i.e. spin−spin (not shown) and spin−lattice (Figure 2c) relaxation times are identical for bare TiO_2 and TiO_2/DA particles. Being localized at least 0.5 nm from the surface in the bulk of the anatase lattice,[31] unpaired electrons on Ti atoms (trapped electrons) do not interact/couple with unpaired electrons of DA^+ radicals. This result suggests that modification of the TiO_2 surface with dopamine would not affect possible reactions of photogenerated electrons, such as reduction of oxygen molecules and formation of superoxide anions as precursors for some of the other ROS,[36] reaction 3.

However, the presence of dopamine on the surface of particles may influence the absorption/desorption processes of O_2 and/or O_2^- and, thus, overall efficiency of charge-transfer reactions, as was shown previously for various organic moieties.[37]

The efficiency of charge separation, the difference in redox properties of localized holes, together with the changes in surface properties between bare and dopamine-modified TiO_2, may all influence the mechanism and yield of ROS formed in photolytic reactions in aerated aqueous solutions.

Suppression of OH Radical Formation from H_2O. In the absence of adsorbed hole scavengers, the formation of OH radicals upon excitation of aqueous TiO_2 undergoes reaction of surface-trapped holes with water molecules, reaction 2.[9−12] In order to examine possible formation of OH radicals upon excitation of TiO_2/DA we have used paramagnetic TEMPOL free radical as a spin probe. The CW EPR spectrum of TEMPOL radical presents a three-line signal characterized by hyperfine splitting $a_N = 17.2$ G, and $g = 2.006$, Figure 3a. TEMPOL nitroxide free radical undergoes reaction with OH radicals resulting in nonparamagnetic species, reaction 8.[38] Thus, by monitoring the decrease in concentration of TEMPOL free

(33) Gallay, R.; van der Klink, J. J.; Moser, J. *Phys. Rev. B* **1986**, *34*, 3060–3068.
(34) Hirsh, D. J.; Beck, W. F.; Innes, J. B.; Brudvig, G. W. *Biochemistry* **1992**, *31*, 532–541.
(35) De la Garza, L.; Saponjic, Z. V.; Dimitrijevic, N. M.; Thurnauer, M. C.; Rajh, T. *J. Phys. Chem. B* **2006**, *110*, 680–686.
(36) Szczepankiewicz, S. H.; Moss, J. A.; Hoffmann, M. R. *J. Phys. Chem. B* **2002**, *106*, 7654–7658.
(37) Berger, T.; Sterrer, M.; Diwald, O.; Knozinger, E. *ChemPhysChem* **2005**, *6*, 2104–2112.
(38) Brezova, V.; Dvoranova, D.; Stasko, A. *Res. Chem. Intermed.* **2007**, *33*, 251–268.

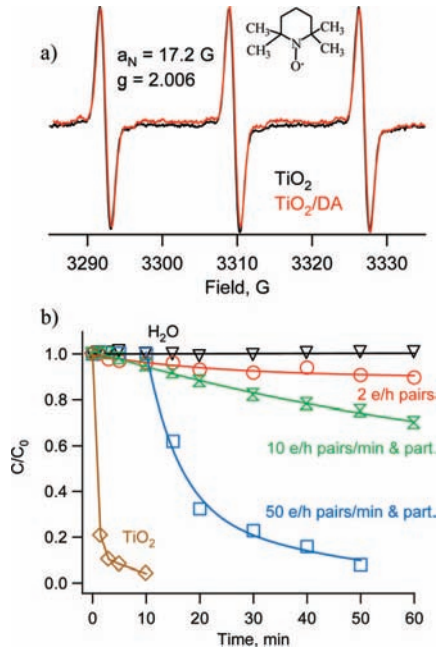

Figure 3. (a) CW EPR spectra of 10 μM TEMPOL radical in aqueous solution of 12.5 mM bare or dopamine-modified TiO_2. Room temperature, microwave power 33 mW, modulation amplitude 1.5 G. (b) Dependence of TEMPOL relative concentration on the illumination time for TiO_2/DA as a function of light intensity (expressed as a nominal number of electron/hole pairs produced per particle per minute). For comparison, the changes in TEMPOL radical concentration for bare TiO_2 is presented (light intensity of 10 e/h pairs per particle and minute).

radicals over time of illumination one can obtain information on the formation of OH radicals.

$$>N-O^{\cdot} + OH \rightarrow N^{+}=O + OH^{-} \quad (8)$$

However, it has been reported that, when bound to the surface of TiO_2 nanoparticles through carboxyl groups, nitroxide probe radicals can be oxidized by trapped holes.[12] For that reason we have avoided spin probes with functional groups capable of specific binding to surface titanium atoms. Additionally, we have established that under the conditions of our experiments, the spectrum of TEMPOL does not change in the presence of either bare or dopamine-modified TiO_2, indicating no preferential adsorption of radicals at the surface of particles, Figure 3a. The concentration of TEMPOL radicals was 10 μM, and titania, 12.5 mM. The photostability of the nitroxide radical was confirmed by illuminating the aqueous solution of TEMPOL (10 μM, pH 3.5) under the highest light intensity used for the particulate solution. These preliminary tests of stability and nonabsorptivity of TEMPOL radicals allowed the use of nitroxide-type spin probes in our experiments. Nevertheless, we cannot rule out some contribution of the reaction of holes trapped at the surface of particles (h_{surf}^-) or on dopamine (DA^+) with TEMPOL, since the oxidation potential for nitroxide radicals is more negative than for water oxidation.[12b]

The changes in TEMPOL concentration over time were determined by measuring room temperature EPR spectra at certain time intervals, while solutions were under continuous UV/vis illumination. Typically, the accumulation of a single spectrum (sweep time) was 42 s in all experiments. The concentration of radicals was determined from a number of spins estimated after double integration of spectra and normalized to the initial concentration (number of spins) of the TEMPOL radical (10 μM). The concentration of TiO_2/DA and TiO_2 was kept constant at 12.5 mM TiO_2 (particulate concentration of $\sim$9 μM), while the intensity of light was changed between experiments. The obtained data are presented in Figure 3b. Contrary to bare titania particles where the presence of OH radicals provides for fast decay of TEMPOL radical concentration, the formation of OH radicals was suppressed in TiO_2/DA, which was further confirmed from the reaction of OH radicals with terephthalic acid (Supporting Information 1).[39] For example, one can compare green line (for TiO_2/DA) with brown line (for bare TiO_2) in Figure 3b, which present decay of TEMPOL radicals under the same conditions/light intensities. A slight decay in radical concentration observed for TiO_2/DA is probably due to the slow charge-transfer reaction of DA^+ with nitroxide radicals. Additionally, the formation of OH radicals from hydrogen peroxide (typically with low yield)[40] could not be ruled out and can contribute to the decay of TEMPOL radicals, reactions 9 and 10.

$$H_2O_2 + O_2^- \rightarrow OH + OH^- + O_2 \quad (9)$$

$$H_2O_2 + e_{tr}^- \rightarrow OH + OH^- \quad (10)$$

Only under extremely high intensity and prolonged time of UV/vis excitation of TiO_2/DA did we observe increased yield of OH radicals formation (see blue line in Figure 3b). Continuous UV/vis illumination of TiO_2/DA provides steady-state conditions, the coincident formation and recombination of photogenerated charges. Thus, by increasing the intensity of light under continuous illumination, at some point in time one can obtain saturated conditions when all dopamine molecules on the surface of particles are oxidized (there are $\sim$400 attached dopamine molecules per 4.5 nm TiO_2 spherical particle). Further UV excitation causes filling of energetically less favorable sites, i.e. the valence band holes that have enough energy to oxidize water and produce OH radicals. On the other hand, illumination with light wavelengths longer than 400 nm produces only DA^+, and despite prolonged intensive illumination, photons do not have enough energy to excite electrons from the valence band of TiO_2, and no OH radicals can be formed in oxidation processes (Supporting Information 2)

Superoxide and Singlet Oxygen Formation. Since shallow lattice-trapped electrons are not affected by the presence of dopamine on the surface of particles, it is expected that they will reduce molecular oxygen to form superoxide anions. Superoxide anion, which undergoes acid−base equilibrium in aqueous solution, is the precursor for singlet oxygen. $^1O_2$ can be formed in low yield by dismutation of two superoxide anions,[15] reaction 5, or at the surface of TiO_2 in reaction of O_2^- with photogenerated holes,[13] reaction 6. The latter reaction depends on the energy (redox potential) of trapped holes, and on the absorptivity of superoxide, and thus can be affected by the presence of dopamine on the surface of particles. Although required energy for formation of singlet oxygen is relatively low, i.e. 0.97 eV (22.5 kcal/mol),[25] holes trapped on dopamine may not provide enough energy to excite oxygen molecules even if reaction between superoxide and DA^+ occurs.

Besides measuring singlet oxygen phosphorescence in near IR as a direct method of detection, there is a range of different fluorescence or spin-trap probes for indirect measurements of

(39) Ishibashi, K.; Fujishima, A.; Watanabe, T.; Hashimoto, K. *J. Photochem. Photobiol., A* **2000**, *134*, 139–142.
(40) (a) Wu, T.; Liu, G.; Zhao, J.; Hidaka, H.; Serpone, N. *J. Phys. Chem. B* **1999**, *103*, 4862–4867. (b) Wu, T.; Liu, G.; Zhao, J.; Hidaka, H.; Serpone, N. *Environ. Sci. Technol.* **1999**, *33*, 1379–1387.

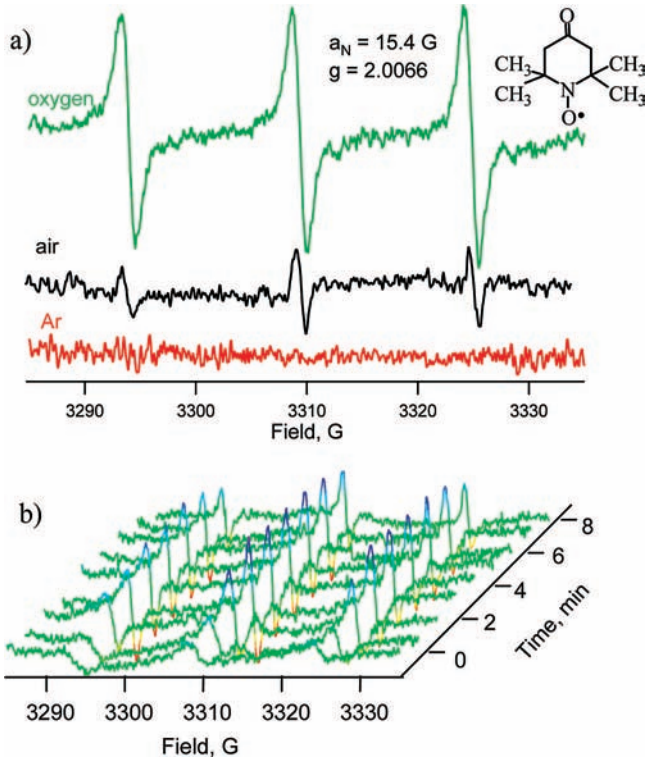

Figure 4. CW EPR spectra of radicals formed (a) after 3 min illumination of 0.1 M TiO_2/DA and 20 mM TEMP aqueous solution saturated with argon (black line), air (red line) and oxygen (green line). (b) EPR spectra measured at different times of continuous UV/vis illumination in oxygenated solution. Microwave power 33 mW, modulation amplitude 1.5 G.

singlet oxygen and/or superoxide. However, they all exhibit limitations, either nonselectivity, or instability (light or oxidative). Thus, we used different complementary probes to test for the formation of superoxide anions and singlet oxygen upon illumination of TiO_2/DA. The spin trap TEMP is generally used as a probe for singlet oxygen in EPR experiments. The reaction of nonparamagnetic species TEMP with singlet oxygen yields formation of a stable radical adduct (nitroxide-type radical), reaction 11.[41] However, there are few reports postulating that O_2^- can contribute to the formation of these radicals, analogous to the reaction of superoxide with tertiary amines.[21,42]

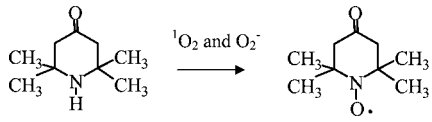

(11)

The formation of nitroxide-type radical, reaction 11, was observed upon excitation of TiO_2/DA in the presence of TEMP at room temperature, Figure 4. The radical exhibits a characteristic EPR spectrum with $g = 2.0066$ and hyperfine splitting $a_N = 15.4$ G. The absence of a signal in Ar-saturated solution, and an increase in radical concentration with an increase of oxygen amount (oxygen- vs air-saturated solutions) confirms involvement of oxygen in formation of these nitroxide radicals. Furthermore, these results demonstrate formation of either O_2^- or $^1O_2$, or both ROS species. The formation of radicals was also detected for bare TiO_2 particles, although fast reaction of

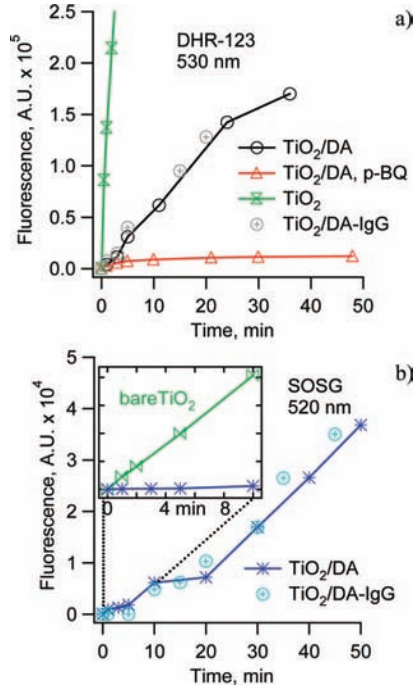

Figure 5. Fluorescence intensity measured after illumination of 12.5 mM TiO_2 and TiO_2/DA (50% coverage) in aerated aqueous solution in the presence of 10 μM dyes: (a) DHR-123 (480 nm excitation, 530 nm emission) and (b) SOSG (480 nm excitation, 520 nm emission). Band-pass filter of 360 nm was used during illumination. Intensity of light corresponds to 2 e/h pairs per particle and minute. Corresponding fluorescence data for 12.5 mM TiO_2/DA-IgG are presented with symbols (⊕). (Inset) Fluorescence intensity of SOSG-$^1O_2$ measured after illumination of 12.5 mM bare TiO_2 under the same conditions.

nitroxide radicals with OH (as demonstrated above) influences the observed kinetics and yield of formation (Supporting Information 3).

In order to distinguish formation of singlet oxygen from superoxide upon illumination of TiO_2/DA, we have used two fluorescent probes, singlet oxygen sensor green (SOSG), a dye which is sensitive only to singlet oxygen, and DHE-123, which is activated by O_2^-/HO_2, H_2O_2 and $^1O_2$.[43] For both dyes, the fluorescence is activated only in reaction with particulate ROS, otherwise they do not exhibit fluorescence. The samples containing nanoparticles and dyes were illuminated in aerated aqueous solution. The 360 nm band-pass filter was used to avoid visible light-induced degradation of dyes, as well as photosensitization of trace amounts of free dopamine, and thus its autoxidation that generates $^1O_2$.[44] The intensity of the incident light was kept low to avoid oxidative reactions. The samples were tested for the presence of ROS at time intervals by measuring fluorescence of activated dyes, and the results are presented in Figure 5, a (for DHR-123) and b (for SOSG). The reaction of DHR-123 with ROS results in the formation of rhodamine 123, and the almost linear increase of its fluorescence with the time of TiO_2/DA illumination is presented in Figure 5a. The addition of a millimolar concentration of *p*-benzoquinone (BQ) was found to suppress formation of rhodamine 123, showing that superoxide anions are the major species

(41) Lion, Y.; Delmelle, M.; Van de Vorst, A. *Nature* **1976**, *263*, 442–443.
(42) Poupko, R.; Rosenthai, I. *J. Phys. Chem.* **1973**, *77*, 1722–1724.
(43) Flors, C.; Fryer, M. J.; Waring, J.; Reeder, B.; Bechtold, U.; Mullineaux, P. M.; Nonell, S.; Wilson, M. T.; Baker, N. R. *J. Exp. Botany* **2006**, *57*, 1725–1734.
(44) Lichszteld, K.; Michalska, T.; Kruk, I. *Z. Phys. Chem.* **1992**, *175*, 117–122.

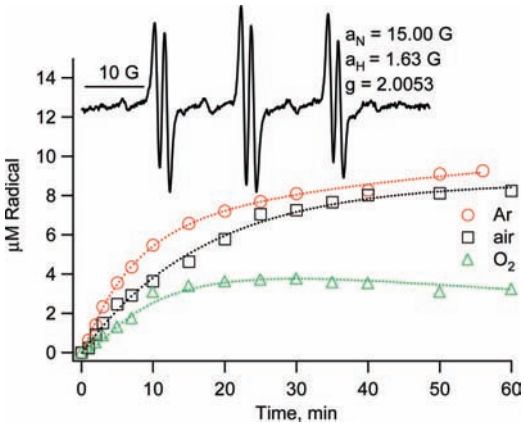

Figure 6. Formation of POBN-OH radicals upon UV illumination of 0.1 M bare TiO_2 and 20 mM POBN aqueous solution saturated with argon (red), air (black), and oxygen (green), pH 3.5. The CW EPR spectrum of POBN-OH radical adduct is presented. Microwave power 33 mW, modulation amplitude 1.5 G.

formed in the reaction of photogenerated electrons with dissolved oxygen. The BQ is a known quencher of superoxide, with the rate constant of 9.6×10^8 M^{-1} s^{-1} for electron transfer reaction 12.[45]

$$BQ + O_2^- \rightarrow BQ^- + O_2 \qquad (12)$$

The formation of singlet oxygen upon excitation of TiO_2/DA is confirmed from SOSG-$^1O_2$ fluorescence measured at 520 nm (480 nm excitation), Figure 5b. The intensity of fluorescence increases with time, reaching a plateau after ~10 min of illumination and then further increases. The shape of the curve suggests second-order reaction of two superoxide anions that requires accumulation of O_2^- at the beginning of illumination, followed by the formation of singlet oxygen through reaction 5. Compared to bare TiO_2, not only the kinetics of $^1O_2$ formation differs, but the yield of singlet oxygen is extremely low in TiO_2/DA system (see Figure 5a, inset). This further suggests that holes trapped at DA are not involved in the formation of singlet oxygen in contrast to the surface-trapped holes of bare TiO_2 particles. Thus, the major route for the formation of singlet oxygen in dopamine-modified TiO_2 is via water-induced dismutation of two superoxide anions.

For bare TiO_2, the main pathway for singlet oxygen formation is reaction of superoxide with trapped holes, reaction 6, as proposed previously.[13] We confirmed this indirectly by measuring fast formation of SOSG-$^1O_2$ (Figure 5b, inset), and/or rhodamine 123 (Figure 5a), and also by measuring the formation of the POBN-OH spin adduct in EPR experiments. The POBN is a spin trap for both OH and HO_2 radicals, the EPR spectra of two different adducts are well resolved.[46] We initially attempted to selectively examine formation of HO_2/O_2^- upon illumination of TiO_2/DA; however, the interference of dopamine radical addition reaction and DA^+ charge-transfer reaction with POBN prevented such measurements (see Supporting Information 4). On the other hand, illumination of bare TiO_2 resulted in the formation of POBN-OH as expected, the radical was identified through g-tensor values and hyperfine splitting, Figure 6. However, the rate of formation and the yield of POBN-OH radical adduct depended on the concentration of dissolved oxygen, the yield being highest in the absence of O_2 (Ar-saturated solution) and decreased with concentration of oxygen. These results can be explained by competition between reactions 2 and 6. Namely, adsorbed superoxide anions, that are produced in reaction of photogenarated electrons with O_2, compete with adsorbed water molecules for photogenarated holes, the higher the concentration of O_2^-, the lower the yield of OH radicals. Additionally, we have shown that singlet oxygen is formed in photolytic reactions from ~5 nm anatase particles.

Finally, we have tested conjugates composed of TiO_2/DA-IgG (antibodies linked to TiO_2 nanoparticles through dopamine) for light-induced formation of superoxide anions and singlet oxygen and have found no significant difference compared to TiO_2/DA (see Figure 5). This opens possibilities for targeting specific cells with adequate antibodies for promoting light-induced cytotoxicity. Specifically, the formation of O_2^-/HO_2 as relatively penetrating radicals does not require deposition of TiO_2/DA-IgG conjugates inside the cell in order to be effective. Similarly, the low yield of $^1O_2$ observed upon illumination of these conjugates may be advantageous, as controlled formation of singlet oxygen (one of the most potent ROS) is prerogative for any bio or medical applications. We are currently conducting in vitro experiments, targeting cytotoxicity upon visible light illumination of TiO_2/DA-IgG conjugates.

Conclusion

Modification of TiO_2 nanoparticles with dopamine results in spatial separation of photogenerated charges, holes localize on dopamine, and electrons localize within the lattice of TiO_2, resulting in suppressed recombination of charges. The spatial separation affects electronic properties and oxidation potential of photogenerated holes, while photogenerated electrons are not affected by the presence of dopamine. However, the formation of ROS that arises from multiple redox chemistries on the surface of particles differs significantly between dopamine-modified and bare TiO_2. We have demonstrated that dopamine radicals, DA^+, on the surface of nanocomposites are not capable of oxidizing water molecules to OH radicals. The major ROS produced upon illumination of TiO_2/DA are superoxide anions, formed in reaction of photogenerated electrons with molecular oxygen. The formation of singlet oxygen in this system probably undergoes dismutation reaction of two O_2^-/HO_2. The measured yield of $^1O_2$ is very low compared to bare TiO_2. The low yield suggests that singlet oxygen is not formed in the reaction of DA^+ with O_2^-, in contrast to bare TiO_2 where the major route for formation of $^1O_2$ is via reaction of photogenerated holes with superoxide anions.

Acknowledgment. The work was performed under the auspices of the U.S. Department of Energy, Office of Basic Energy Sciences under Contract No. DE-AC02-06CH11357.

Supporting Information Available: EPR spectra and kinetics of decay and formation of nitroxide radicals upon illumination of TiO_2/DA, and the fluorescence of 2-hydroxyterephthalic acid formed in the reaction of OH radicals with terephthalic acid upon illumination of bare TiO_2 nanoparticles. This material is available free of charge via the Internet at http://pubs.acs.org.

JA807654K

(45) Bandara, J.; Kiwi, J. *New J. Chem.* **1999**, *23*, 717–724.
(46) Buettner, G. R. *Free Radical Biol. Med.* **1987**, *3*, 259–303.